Volume 16
Number 20
28 May 2024
Pages 3157–3298

Analytical Methods

rsc.li/methods

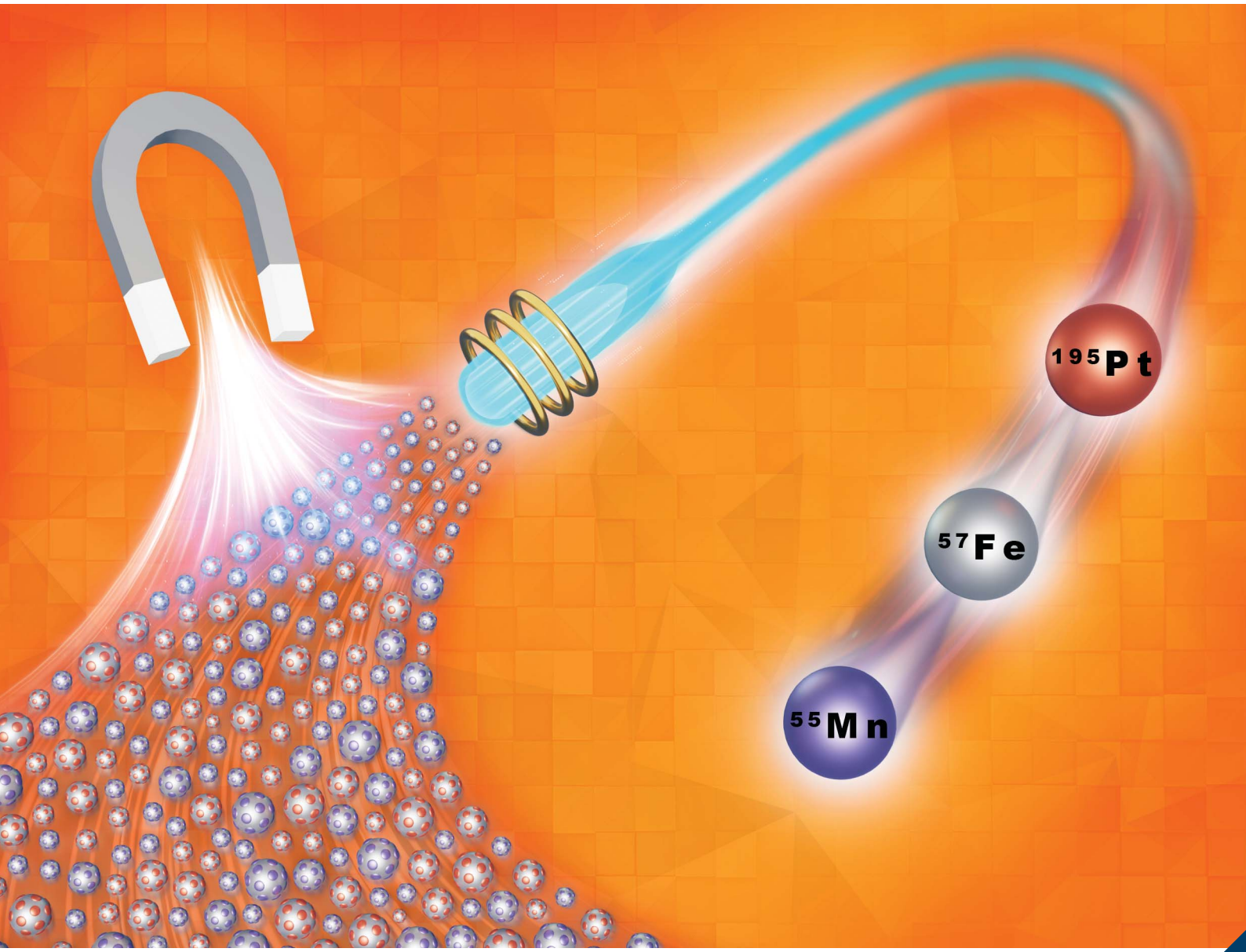

ISSN 1759-9679

ROYAL SOCIETY OF CHEMISTRY

PAPER
Benjamin T. Manard, Hunter B. Andrews *et al.*
Quantifying platinum binding on protein-functionalized magnetic microparticles using single particle-ICP-TOF-MS

Indexed in Medline!

Analytical Methods

ROYAL SOCIETY OF CHEMISTRY

PAPER

View Article Online
View Journal | View Issue

Cite this: *Anal. Methods*, 2024, **16**, 3192

Quantifying platinum binding on protein-functionalized magnetic microparticles using single particle-ICP-TOF-MS†‡

Veronica C. Bradley, [a] Benjamin T. Manard, *[a] Lyndsey Hendriks, [b] Daniel R. Dunlap,[a] Amber N. Bible,[c] Ada Sedova, [c] Patricia Saint-Vincent,[c] Brian C. Sanders [c] and Hunter B. Andrews *[d]

This work describes an analytical procedure, single particle-inductively coupled plasma-time-of-flight-mass spectrometry (SP-ICP-TOF-MS), that was developed to determine the platinum binding efficiency of protein-coated magnetic microparticles. SP-ICP-TOF-MS is advantageous due to its ability to quasi-simultaneously detect all nuclides (^{7}Li–^{242}Pu), allowing for both platinum and iron (composition of magnetic microparticles) to be measured concurrently. This method subsequently allows for the differentiation between bound and unbound platinum. The 1 μm magnetic microparticles were fully characterized for their iron concentration, particle concentration, and trace element composition by bulk digestion-ICP-MS and SP-ICP-TOF-MS. The results of both approaches agreed with the certificate values. Using the single particle methodology the platinum loading was quantified to be to 0.18 ± 0.02 fg per particle and 0.32 ± 0.02 fg per particle, for the streptavidin-coated and azurin-coated microparticles, respectively. Both streptavidin-coated and the azurin-coated microparticles had a particle–platinum association of >65%. Platinum bound samples were also analyzed *via* bulk digestion-based ICP-MS. The bulk ICP-MS results overestimated platinum loading due to free platinum in the samples. This highlights the importance of single particle analysis for a closer inspection of platinum binding performance. The SP-ICP-TOF-MS approach offers advantages over typical bulk digestion methods by eliminating laborious sample preparation, enabling differentiation between bound/unbound platinum in a solution, and quantification of platinum on a particle-by-particle basis. The procedure presented here enables quantification of metal content per particle, which could be broadly implemented for other single particle applications.

Received 14th February 2024
Accepted 13th April 2024

DOI: 10.1039/d4ay00268g

rsc.li/methods

Introduction

Platinum (Pt) metal and Pt-based materials and compounds are essential to numerous applications including catalysts for clean energy, industrial production of materials such as silicones, and use in medicine and medical devices. Because of these roles, Pt and other Pt-group metals (PGMs), like palladium and iridium have been identified as critical materials for secure energy and economic future.[1–3] The catalytic properties of PGMs warrant their use in automotive catalytic converters to reduce emissions, as well as in water electrolysis applications.[3–5] Deposits of Pt in quantities that are economic for mining are rare, only one mine in the US produces non-byproduct Pt.[6] Accordingly, recycling of Pt and PGMs is crucial in keeping up with demand for these elements. Notably, proteins and other biological materials such as chitosan have been studied as sorbents for various metals including the PGMs.[7,8] Pt is also known to intercalate into DNA and has been leveraged for chemotherapeutics; however, PGMs and other heavy metals can be extremely toxic.[9,10] Given the critical need for PGMs, their essential roles in catalysis, and their diverse biological activity, it is necessary to better understand the interactions of Pt with biological materials such as proteins.

[a]*Chemical Sciences Division, Oak Ridge National Laboratory, Oak Ridge, TN, USA. E-mail: manardbt@ornl.gov*

[b]*Tofwerk AG, Thun, Switzerland*

[c]*Biosciences Division, Oak Ridge National Laboratory Oak Ridge, TN, USA*

[d]*Radioisotope Science and Technology Division, Oak Ridge National Laboratory Oak Ridge, TN, USA. E-mail: andrewshb@ornl.gov*

‡ Electronic supplementary information (ESI) available. See DOI: https://doi.org/10.1039/d4ay00268g

Magnetic nano- and microparticles have been studied in recent years for their utility in separations and as scaffolds for biological sensors.[11–13] These particles offer advantages including relative ease of removal from complex matrices without filtration or centrifugation, they can be readily functionalized with a wide range of different groups, and they can be regenerated and reused.[14] Hamza *et al.* used magnetite-chitosan nanoparticles functionalized with amidoxime and hydrazinyl amine groups to recover U and Zr from acidic solutions.[15] Other research has explored eliminating pollutants during wastewater treatment through adsorption to functionalized $CoFe_2O_4$ nanoparticles[16] and actinide capture with magnetite nanoparticles functionalized with TODGA and HDEHP.[17] It has been shown that after analyte adsorption, particles can be stripped and reused, which decreased the cost of their use in separations.[16] A number of analytical strategies were employed in these studies to find how well the functionalized particles worked for removing analytes, including using inductively coupled plasma-optical emission spectroscopy (ICP-OES) to measure the analyte concentration before the addition of the magnetic particles, and then again after their removal.[15,18] While this method works well to determine the amount of material taken up by the particles on a bulk scale, it cannot give any information about binding properties on an individual particle level.

Single particle – inductively coupled plasma – mass spectrometry (SP-ICP-MS) is getting increased attention, particularly in the fields of nanomaterials, environmental chemistry, and medicinal chemistry, due to the technique's ability to distinguish dissolved background signal from particle signal and characterize particles on a particle basis.[19,20] Operating an ICP-MS in single-particle mode requires transient signal monitoring and fast acquisition times.[20–22] An instrument with a time-of-flight (TOF) mass analyzer is ideal for single particle-based applications as they have very fast integration times down to tens of μs and can monitor all nuclides in the mass range ~7–275 amu quasi-simultaneously.[23] Because of these advantages, SP-ICP-TOF-MS has been used for a wide range of applications over the past few years including environmental analysis,[24,25] investigation of interstellar particles,[26] detection of microplastics,[27,28] and both the detection and characterization of nanoparticles.[12,29,30] As an extension of SP-ICP-TOF-MS, the application of the technique to measure endogenous elements and/or metal tagged single cells has quickly become a growing field.[31–33] In order to quantify single particles and single cells, Pace *et al.* developed a quantification method that relies on the use of nanoparticle standards to correlate calibration curves to particle signals for mass determination.[22] This technique is useful for applications where the analyte particles and standard particles are a similar size, it is not ideal for applications when analyte particles (*e.g.*, single cells) are much larger than the standards, as transport efficiency is size dependent.[34] In these instances when cells fall on the 3–5 μm scale, a larger particle standard on a similar scale would be of great interest.

Azurin (Az) is a well-characterized protein and has been used in diverse applications including biological electron transfer studies, protein engineering, and has been shown to maintain its function when immobilized.[35–37] Importantly, one study showed that a single mutation of histidine 117 to glycine (H117G), allows Az to bind $K_2[PtCl_4]$ and $K_2[PdCl_4]$.[38] With this in mind, we expressed the H117G azurin with streptavidin (SA) affinity tag and immobilized it to SA-coated magnetic Fe microparticles to capture $K_2[PtCl_4]$ in solution. Importantly, this study focuses on the development of an analytical method to measure the amount of metal binding to protein-functionalized microparticles through SP-ICP-TOF-MS. Studying the optimization of Pt association on azurin requires an analytical method with high sample-throughput. To achieve this, an automated sample introduction system was employed, which included a mixing procedure to ensure particles were suspended in buffer over the course of long analysis times (>5 h). The sample, after mixing, was injected into a high efficiency nebulizer and spray chamber which have a transport efficiency of >80% (for 50 nm Au particles), which maximizes sample transport during analysis. Az-coated microparticles were compared to SA-coated microparticles to demonstrate the ability to quantify Pt binding efficiency of various proteins using SP-ICP-TOF-MS.

Materials and methods

Materials and reagents

All dilutions were matrix matched in 50 mM ammonium acetate buffer (pH ~ 7.4) following an investigation of matrix effects on instrument sensitivity. To explore the buffer effects on the ability to accurately and precisely determine the Pt concentrations in these experiments, the authors doped 1 ng mL^{-1} (single element standard, High Purity Standards, Charleston, SC, USA) in various buffers including ammonium acetate, 3-(*N*-morpholino)propanesulfonic acid (MOPS), phosphate buffered saline (PBS at 0.1 M and 1 M), and 4-(2-hydroxyethyl)-1-piperazineethanesulfonic acid (HEPES). It was determined that there was a drastic reduction (90, 69, and 54%) in Pt sensitivity for the 1 M PBS, MOPS, and 0.1 M PBS, respectively. HEPS was less drastic with a 8.4% reduction in sensitivity while the ammonium acetate reduction was negligible. Images of the ICP under the different buffer can be seen in the ESI (Fig. S1‡).

Calibration standards with final concentrations of 1, 5, and 10 ng mL^{-1} were prepared gravimetrically from single element stock solutions (10 μg mL^{-1}) of Au, Fe, and Pt from High Purity Standards. Monodispersed gold nanospheres with 100 nm diameter (102.2 ± 4.2 nm) were obtained from nanoComposix (Fortis Life Sciences, San Diego, CA, USA) and utilized as particle standards. Dynabeads MyOne Streptavidin T1 microparticles were purchased from Thermo Fisher Scientific (Waltham, MA, USA). The T1 microparticles (1 ± 0.05 μm) are superparamagnetic consisting of a mixture of maghemite (γ-Fe_2O_3) and magnetite (Fe_3O_4) with a Fe content of 26% and are supplied at a particle concentration of 7–10 × 10^9 particles per mL. Optima grade nitric acid and hydrochloric acid (Fisher Scientific, Pittsburg, PA, USA) were used in digesting samples for bulk analysis.

Protein expression and purification

The Az single mutant H117G was synthesized and cloned into pET-51b(+) by GenScript. For each sample set ($n = 3$) BL21 DE3 *E. coli* were transformed with the H117G vector and a single colony was selected for growth in Luria-Bertani (LB) media (1 mL overnight starter cultures, 100 μg mL^{-1} ampicillin). The starter cultures were used to inoculate 20 mL LB (100 μg mL^{-1} ampicillin) that was grown for 3 h at 250 rotations per min (RPM), 37 °C. After 3 h, IPTG was added to a final concentration of 1 mM and the temperature was lowered to 25 °C and mixed at 250 RPM overnight. The cells were pelleted at 100 00×*g* for 10 minutes, then the supernatant was discarded. Lysis was performed with Thermo Scientific B-PER II Bacterial Protein Extraction Reagent (2X) at a volume of 5 mL for 20 minutes while rocking at room temperature. The cell lysate was centrifuged at 100 00×*g* for 10 minutes to afford a clear lysate. Lysates were heat treated at 50 °C for 1 h followed by centrifugation (10 min, 100 00×*g*) to remove endogenous *E. coli* proteins. Cell lysates were combined with Dynabeads™ MyOne™ Streptavidin T1 magnetic microparticles for 30 min at room temperature and then washed 3× with PBS (250 mM NaCl, 0.1% Tween-20). Microparticles were boiled in NuPAGE™ to release bound protein and confirm selective H117G azurin binding by SDS-PAGE (Fig. S2‡).

H117G azurin and Pt loading on to microparticles

Cell lysates were generated as described above. The lysates were heated at 50 °C for 1 hour before centrifugation (100 00×*g*, 20 min). Next, we mixed 2 mL lysate with 700 μL of stock microparticles at RT for 30 minutes, washing 3× with PBS (250 mM NaCl, 0.1% Tween-20) then replacing with just PBS before adding $K_2[PtCl_4]$. A solution of $K_2[PtCl_4]$ (10 mM) in water was prepared immediately prior to addition to H117G azurin-bound microparticles at a 1 mM final concentration of $K_2[PtCl_4]$. Microparticles were incubated at 50 °C for 1.5 hours followed by washing 2× in PBS with tween, then 2× with ammonium acetate (50 mM, pH 7). Control microparticles with no H117G azurin, and with no $K_2[PtCl_4]$ added were handled analogously as above. After washing, samples were vortexed for 30 s to ensure uniform particle suspension, then diluted in 50 mM ammonium acetate buffer (pH ∼ 7.4) such that there were approximately 7000 microparticles mL^{-1}.

Scanning electron microscopy

Images were collected using a Zeiss Gemini 460 (SEM, Oberkochen, Germany) at 2 kV with a working distance of 8 mm and a probe current of 1.3 nA. Samples were diluted in water and deposited in 1 μL aliquots onto a vitreous carbon planchet (Ted Pella, Inc, Redding, California, USA). Secondary electron micrographs were taken of the microparticles on the carbon planchet at 5000× and 275 70× magnifications.

Single particle-ICP-TOF-MS

An icpTOF R (TOFWERK AG, Thun, Switzerland) was integrated with a microFAST SC sample introduction system from Elemental Scientific Inc (ESI, Omaha, NE, USA) for high throughput analysis.[29] The operating conditions of the ICP-TOF-MS can be found in Table 1. The ICP-TOF-MS was operated in collision cell technology (CCT) mode using ultra high purity (99.999%) H_2 and He gases (Airgas, Radnor, Pa, USA) to remove ArO interferences at m/z 56 and 57. The single particle data was acquired and processed using the particle module in TOFpilot v2.12.0 (TOFWERK AG, Switzerland). The compound Poisson thresholding[39] was used to identify particle events from the background and the quantification followed the approach developed by Pace *et al.* using the particle size method for the determination of the transport efficiency.[22]

Table 1 SP-ICP-TOF-MS operating conditions

Parameter	Value
H_2 flow (collision cell)	2 mL min^{-1}
He flow (collision cell)	1 mL min^{-1}
Nebulizer gas (Ar)	0.45 L min^{-1}
Add gas (Ar)	0.38 L min^{-1}
Sample uptake rate	10 μL min^{-1}
Injection volume	100 μL
Sampling depth	5 mm
Plasma power	1550 W
MCP target	2520 V
Single ion signal	2.41 mV ns
Acquisition time	1 s (liquid)
	2 ms (particle)

The microFAST SC autosampler sequence was created as described previously[29] in a study characterizing nanoparticles. Briefly, the autosampler probe goes into the sample and mixes *via* high speed (3000 μL min^{-1}) alternating pumping of the sample using a syringe pump. Following mixing, the sample is delivered into an injection loop (100 μL) for precise sample loading into the ICP introduction system. Between each sample analysis a two-step probe rinse is performed, as well as a blank (DI) sample which follows the same introduction protocol. A CytoNeb50 nebulizer (ESI) and a CytoSpray spray chamber (ESI, SC-CytoC-73) were utilized. This sample introduction system is designed to have high transport efficiency for use in single particle applications and provide automated sample introduction. Typical transport efficiency for 100 nm Au nanoparticles was determined to be >65% for the setup in this study. This value falls below that of previous studies on the same system, but was expected due to the change in sample matrix from milliQ to ammonium acetate. After a delay for sample uptake, data was acquired for 300 s with a 2 ms integration time. The single particle analysis setup is shown in Fig. 1.

Bulk-ICP-MS analysis

Prior to bulk digestion ICP-MS analysis, the stock was vortexed for 30 s to ensure complete suspension. A gravimetrically prepared aliquot (10 μL) of the magnetic microparticle suspension was digested in 5 mL of 6 M HCl in a 7 mL Savillex Vial, at 120 °C, for 12 h. Then, a 100× dilution was performed on the dissolved samples with 2% HNO_3. These samples were then analyzed against an external calibration curve on an iCAP TQ-ICP-MS (Thermo Scientific, Bremen, Germany). The

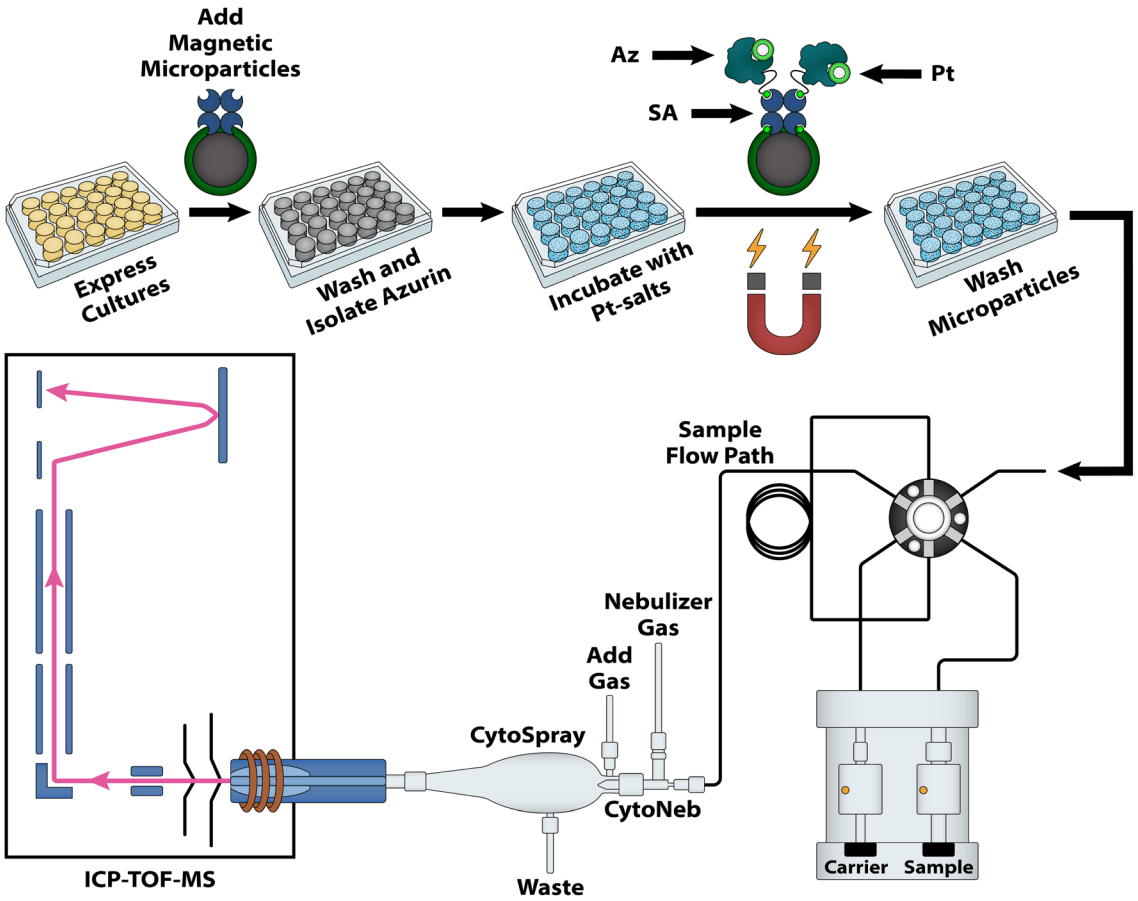

Fig. 1 Diagram of experimental workflow and SP-ICP-TOF-MS system. SA and Az refer to streptavidin and azurin, respectively.

measurement was performed in kinetic energy discrimination mode with a He collision gas.

Results and discussion

Analysis and characterization of magnetic Fe microparticle substrate

The experiments evaluated in this study rely on the SA-coated Fe microparticles as a substrate for Pt binding. It is crucial to have a well characterized, and consistently sized, substrate for efficiently evaluating metal binding performance of various proteins. If the microparticles are not monodisperse it could lead to difficulties in deciphering differences between different proteins. Therefore, it was essential to focus the initial efforts of this study on the characterization of these microparticles. The certified size of the magnetic Fe microparticles is 1 ± 0.05 μm. Fig. 2 shows SEM images of a dried aliquot of the magnetic microparticle suspension. The microparticles appear very monodispersed and a closer examination shows the particles of the anticipated scale (Fig. 2). Energy dispersive X-ray spectroscopy maps highlighting Fe and O content of an aliquot of microparticles is provided in Fig. S3.‡

According to the manufacturer information, the stock solution contains 10 mg particles per mL and the Fe content in the microparticles is 26%, meaning there should be 2.6 mg Fe

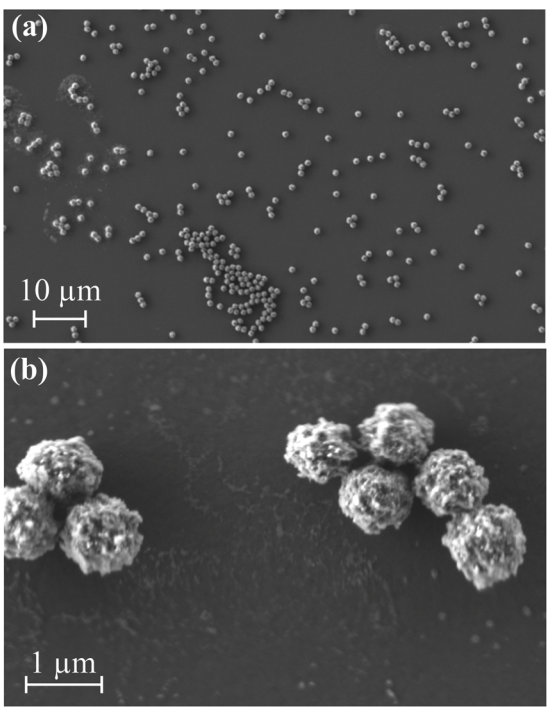

Fig. 2 SEM images of the magnetic Fe microparticles showing (a) a monodispersed population and (b) the anticipated 1 μm size.

Table 2 Comparison of certificate, bulk, and single particle characterization values of the magnetic Fe microparticles

	Certificate	Bulk	Single particle
Fe concentration (mg mL^{-1})	2.6	2.55 ± 0.20	2.42 ± 0.49[a]
Particle concentration	8.5 ± 1.5 × 10^9	—	8.3 ± 0.4 × 10^{9a}
Fe loading (fg per bead)	306 ± 54[a]	302 ± 53[a]	292 ± 59

[a] Calculated with assumptions.

per mL in the stock. Initially, the microparticles were analyzed using bulk-ICP-MS to determine the Fe concentration as well as trace element impurities. The Fe concentration of the stock microparticle solution was determined to be 2.55 ± 0.20 mg Fe per g using external calibration bulk-ICP-MS, which agrees well with the manufacturer information (Table 2). A full trace element analysis was conducted on the digested microparticles, and two impurities were detected: 7.8 ± 0.62 μg Mn per g and 0.56 ± 0.05 μg V per g.

For SP-ICP-TOF-MS analysis, the microparticles were diluted 100 000× (to a concentration of 7–10 × 10^4 particles per mL) to allow for the detection of individual microparticles. The SP-ICP-TOF-MS time trace from a single injection of Fe microparticles is shown in Fig. 3. The microparticles produce relatively consistent signal intensities with relative standard deviation (RSD) values of 20% and 14% (n = 28 799), for ^{56}Fe and ^{57}Fe, respectively, which is further indication of a uniform size distribution.[29]

An added benefit of the ICP-TOF-MS is that all nuclides are monitored quasi-simultaneously, thereby allowing the determination of the complete composition of the microparticles. Upon investigation of all measured isotopes, the Mn trace impurity was identified; however, the V trace impurity was below detection limits. The Mn signal was utilized as an additional metric to differentiate particle events from background during data analysis.

The Fe concentration in the stock solution cannot be calculated directly from the SP-ICP-TOF-MS to compare with the bulk-ICP-MS measurements. However, it can be estimated under the assumption of a constant transport efficiency. Using a measured particle concentration of 8.3 ± 0.4 × 10^9 particles per mL (based on Au transport efficiency), and the Fe loading per particle (detailed below), the determined Fe concentration using SP-ICP-TOF-MS data was 2.42 ± 0.49 mg Fe per mL. The certificate, bulk-ICP-MS, and SP-ICP-TOF-MS values are compared in Table 2. Interestingly, both the particle concentration and Fe concentration estimated from the SP-ICP-TOF-MS measurements, using the assumption of a consistent transport efficiency, agree well with the certificate values.

While the certificate and bulk-ICP-MS do not provide a direct measurement of the Fe mass per particle, yet it could be calculated using the certificate particle concentration. Here, the mass of Fe in the average microparticle was estimated to be 306 ± 54 fg and 302 ± 53 fg for the certificate and bulk-ICP-MS, respectively. The SP-ICP-TOF-MS provides the opportunity to

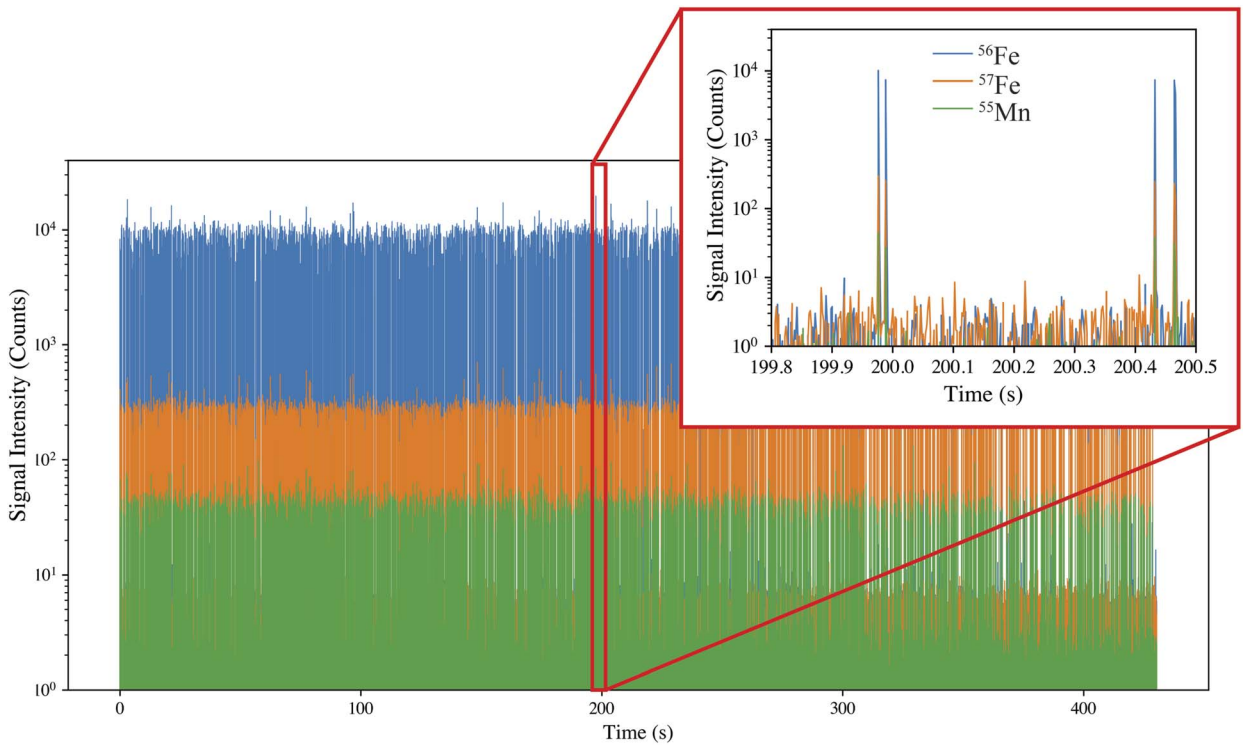

Fig. 3 Transient SP-ICP-TOF-MS signal (^{56}Fe, ^{57}Fe, and ^{55}Mn) of streptavidin-coated magnetic Fe microparticles over the course of a single injection showing the consistent signal intensity. The insert plot provides a closer look at the concurrent isotopic signals during an event.

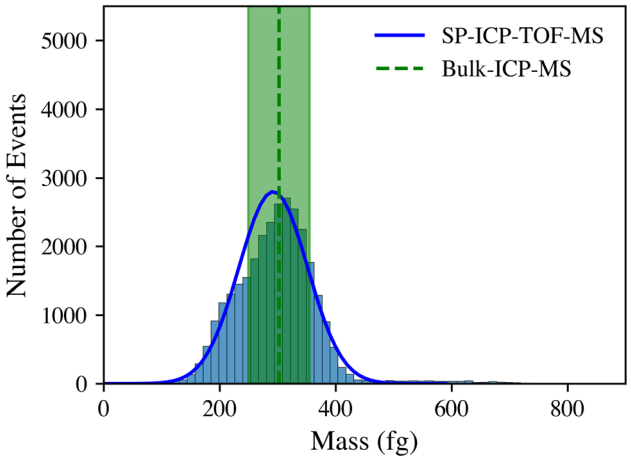

Fig. 4 Total Fe mass distribution as determined using the recorded signals for ^{56}Fe from single particle analysis shown with a Gaussian fit. The average bulk-ICP-MS values are superimposed for comparison.

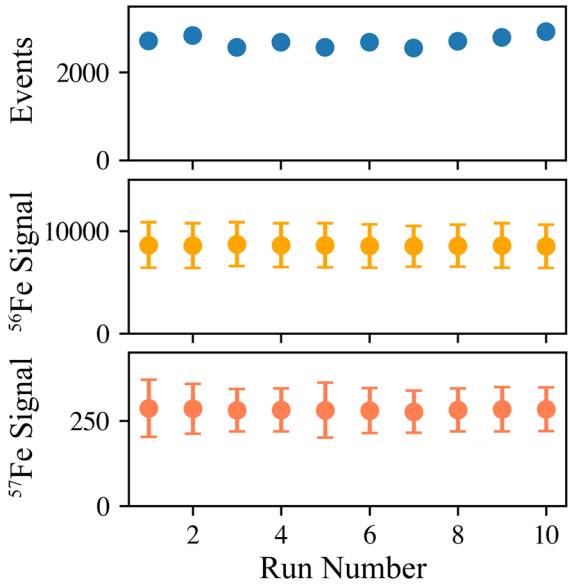

Fig. 5 Long term stability and reproducibility of SP-ICP-TOF-MS measurements for the Fe microparticles over 10 injections (~4 hours total analysis time).

calculate the Fe loading directly by quantifying the Fe in each event. The Fe content in the particles was found to be 292 ± 59 fg, based on ^{56}Fe recorded signals. The SP-ICP-TOF-MS data agreed well with the bulk mass within uncertainty; the single particle value was compared to bulk through zeta scores, which were found to be 0.002. Scores within ±1 are generally considered highly acceptable. For the purposes of this study, we focused on the Fe mass calculations determined from the ^{56}Fe recorded signals because the low natural abundance of ^{57}Fe (~2%), which leads to lower counting statistics, especially in the calibration curve. The total Fe mass distributions based on the ^{56}Fe recorded signals for the unfunctionalized microparticles are shown in Fig. 4. A small, second population was seen at approximately 520–580 fg. This can be attributed to double events. Indeed, when analyzing suspensions with SP-ICP-TOF-MS, two or more particles may occasionally enter the plasma concurrently, leading to a single peak representing multiple particles. To evaluate metal loadings on a single particle basis, all analysis was made with double events filtered out. The bulk-ICP-MS value is superimposed on the SP-ICP-TOF-MS mass measurements in Fig. 4 and are compared in Table 2. These values agree with the single particle data within uncertainty, showing that although each analysis method provides different data in different formats, they are all congruent and accurate analytical techniques.

Sample reproducibility

For high-throughput, large sample population experiments it is essential that the SP-ICP-TOF-MS measurement be reproducible and capable of consistent measurements over the course of hours. It is not unreasonable to anticipate sample batches for the analysis of protein-functionalized microparticles for metal binding being prepared within 96-well plates which indicated the necessity for automated sampling. Recently, in the realm of SP-ICP-MS, much effort has been focused on automated efforts.[20,29,40] In terms of automated sample analysis, considerations should be placed on sample mixing, sample stability, and consistent injections, particularly when considering long term sequences. To test the robustness and reproducibility of the method, a 4 h sequence was performed such that 10 injections, with subsequent rinsing steps, and standards were analyzed. Fig. 5 shows the number of magnetic Fe microparticles detected, along with the Fe isotope signals, over the course of the 10 injections. The microparticles showed high stability and reproducibility over the course of 10 injections (for a total analysis time of ~4 h). The number of particles detected was 2700 ± 120 for the replicate injections and the average signal for ^{56}Fe through the 10 injections was 8598 ± 57 counts. The number of particles detected over the 10 runs only showed a 4.4% RSD and the ^{56}Fe signal had a 0.6% RSD, indicating a consistent transport efficiency and effective automated mixing. This stability over time shows the robustness of the SP-ICP-TOF-MS method and the benefit of the autosampler mixing prior to injection.

Before continuing with the core of this study, assessing the binding performance, a brief divergence is warranted here to consider the potential of these magnetic Fe microparticles for other applications. Indeed, following their thorough characterization, these microparticles may be of interest to the single cell analytical community where a larger particle standard on the μm scale would be advantageous. Commonly used particle standards used for the determination of the transport efficiency are in the nano-size range like the Au nanoparticles used here and these may not accurately represent the behaviour of the target analyte, leading to concerns about size-dependent transport efficiency biases. Recent studies have reported different transport efficiencies for NPs standard and subsequent samples under analysis (*i.e.*, cells[31–33] and microplastics[27,41]) using the particle frequency method.[22] This size-dependent transport efficiency bias has been reported for

particles larger than 3–5 μm,[33] and proves that the existing nanoparticle standards (nm-size range) do not adequately address the disparities in size when applied to micron-sized cells. These observations suggest the need for a well-characterized micron-size standard for the analysis of micron sized-entities. While commercially available options such as Fluidigm's EQ Calibration Beads offer potential solutions, it is important to note their restricted accessibility, primarily being available to users of Fluidigm's CyTOF systems. Therefore, there remains a demand for micron-sized particles standards that are accessible to researchers utilizing various mass spectrometry platforms. Hence, to address this gap, one may envision using the now well-characterized Fe microparticles as a standard for ICP-MS analysis of single-cell and single-particle micron-sized species.

Pt binding measurements

With the magnetic microparticles characterized, the next measurements were performed to quantify the Pt binding efficiency of H117G azurin (Az)-coated *versus* the only streptavidin (SA)-coated microparticles. Triplicate samples of both Az- and SA-coated microparticles were exposed to $K_2[PtCl_4]$, washed, and then analyzed using SP-ICP-TOF-MS and bulk-ICP-MS. Table 3 provides a comparison of ICP-TOF-MS and TQ-ICP-MS sensitivities, along with the SP-ICP-TOF-MS method figures of merit. An example SP-ICP-TOF-MS transient of the Az-coated microparticles is shown in Fig. 6. The insert plot of Fig. 6 highlights the SP-ICP-TOF-MS ability to discern microparticles with and without Pt.

First, the Fe–Pt association was determined by investigating the population of Fe microparticle events and comparing the number of events with and without bound Pt signals. The 1 μm Az-coated particles were found to have a binding association of $71 \pm 3\%$ ($n = 3$) while SA-coated particles had a $65 \pm 3\%$ ($n = 3$) association. The high association of the SA-coated particles and Pt is likely due to nonspecific binding of Pt with streptavidin. It is important to note the analysis of event level information like association is possible due to the quasi-simultaneous nuclide measurements granted by the ICP-TOF-MS.

To further investigate the performance of the protein-coated microparticles, the Pt loading was investigated. With use of Pt external calibration standards, the mass of Pt per microparticle was determined using the ^{194}Pt, ^{195}Pt, and ^{196}Pt signals. The Pt mass calculated using each isotope was very consistent with an average % RSD of 0.6% across all samples. Taking the average of the Pt loadings calculated from each isotopic signal, the Az-

Table 3 Comparison of instrument sensitivities and figures of merit

	ICP-TOF-MS[a]	TQ-ICP-MS	SP-ICP-TOF-MS[a]
Sensitivity	1.50×10^4 (cps ppb^{-1})	1.2×10^5 (cps ppb^{-1})	1.14×10^{17} (counts per g)
LOD	1.28×10^{-3} (ppb)	8.9×10^{-4} (ppb)	4.63×10^{-17} (g)

[a] ICP-TOF-MS measurements were performed using ammonium acetate buffer.

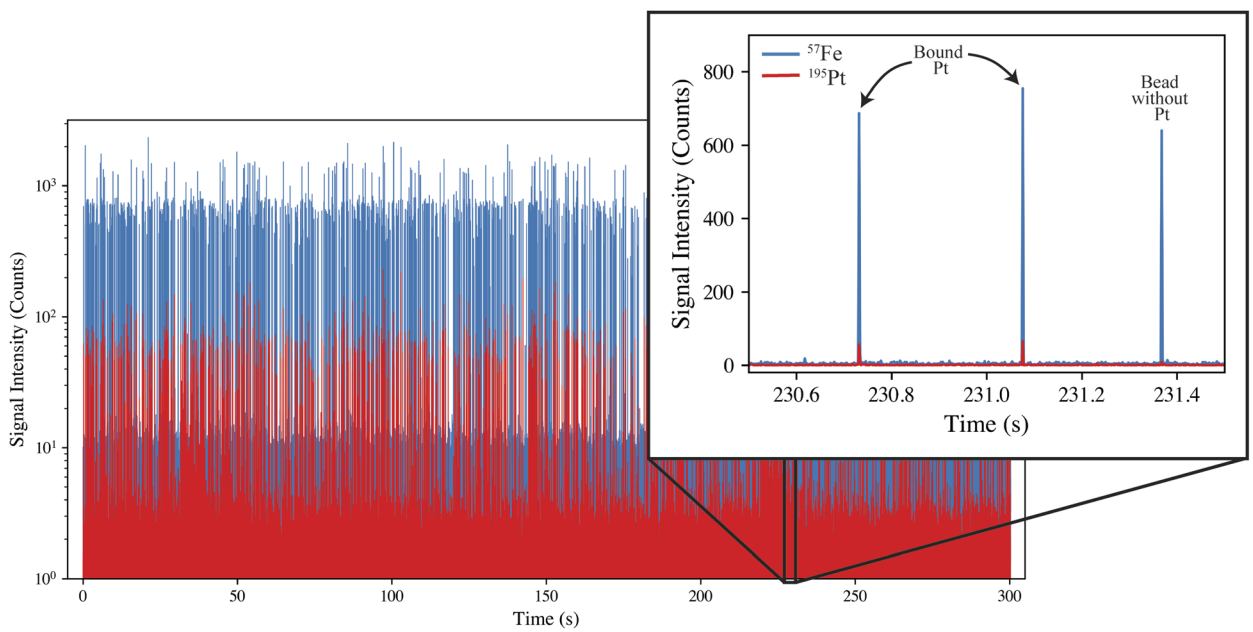

Fig. 6 Transient SP-ICP-TOF-MS signal (^{57}Fe and ^{195}Pt) of the mutant azurin functionalized microparticles over the course of a single injection. Additional time traces for Fe, Mn, and Pt isotopes are not shown for visual simplicity. The insert plot provides a closer look at the ability to distinguish microparticles with and without bound Pt.

coated samples were determined to have an average of 0.32 ± 0.02 fg Pt per microparticle, while the SA-coated microparticles had an average of 0.18 ± 0.02 fg Pt per microparticle. Consequently, the Pt loading on an individual microparticle is much higher for mutant azurin (84%) compared to streptavidin alone.

The microparticle manufacturer provides a loading range for free biotin of 950–1500 pmol mg^{-1}. Under the assumption that azurin binds within this range, and assuming a 1 : 1 stoichiometry for Pt : Az, the theoretical binding of Pt to Az-coated beads would be 0.04–0.13 fg Pt per microparticle. Based on the loadings calculated using SP-ICP-TOF-MS, the estimated stoichiometry of Pt atoms bound to streptavidin ranges from 1.4–4.5 Pt atoms per streptavidin protein. The azurin analysis is more challenging since we cannot know if the amount of Pt bound is simply additive to that of streptavidin or if azurin precludes binding of Pt to the streptavidin. If the former, then we observe 1.1–3.5 Pt atoms per azurin protein that is comparable to the anticipated 1 : 1 stoichiometry.

When comparative Pt loading values were calculated with bulk-ICP-MS measurements, assuming 8.5×10^9 particles per mL, the Pt loading was estimated to be 0.7 ± 0.2 fg Pt per microparticle and 0.4 ± 0.1 fg Pt per microparticle for the Az- and SA-coated microparticles, respectively. While the SP- and bulk-ICP-MS data do not match exactly, they follow a similar trend in which Az-coated microparticles can capture approximately 180% the amount of Pt per microparticle compared to streptavidin alone. The interactions of Pt with both SA and SA-Az appear to be non-specific because a molar excess of Pt per protein is bound in both cases, however, selective binding (1 : 1 Pt : Az) would be discernible with this method. The SP-ICP-MS and bulk-ICP-MS values for SA- and Az-coated samples are compared in Table 4.

The bulk-ICP-MS results yielded larger Pt loadings for both the Az- and SA-coated samples than the SP-ICP-TOF-MS values. The likely explanation for this difference is due to free Pt. Since bulk digestion results in only a solution concentration of Fe and Pt, it does not take into consideration either the free Pt or Fe microparticles without bound Pt (see inset of Fig. 6). Additionally, samples for SP-ICP-TOF-MS analysis undergo further dilution which would decrease any ionic Pt levels in the single particle data that otherwise inflates the bulk values. The impact of distinguishing free and bound Pt on measured Pt binding levels highlights the importance of analysis on a particle by particle basis using SP-ICP-TOF-MS for quantifying metal binding to protein-functionalized magnetic microparticles. Lastly, the SP-ICP-TOF-MS measurement in this study provides a control for the experimental procedure such that if the magnetic microparticles are inadequately washed an elevated Pt background will be detected; this would not be possible with bulk-ICP-MS.

Table 4 Comparison of SP-ICP-TOF-MS and bulk-ICP-MS Pt loading values before and after applying the Fe–Pt association rates to account for unbound events[a]

	Fe–Pt association	Pt loading (fg per particle)	
	SP-ICP-TOF-MS	SP-ICP-TOF-MS	Bulk-ICP-MS
SA-coated	65 ± 3%	0.18 ± 0.02	0.4 ± 0.1
Az-coated	71 ± 3%	0.32 ± 0.02	0.7 ± 0.2

[a] SP-ICP-TOF-MS $n = 3$.

Conclusions

In this study, a procedure was developed to measure Pt loading on magnetic microparticles functionalized with proteins. First, the magnetic microparticles were characterized using both SP-ICP-TOF-MS and bulk-ICP-MS. The substrate microparticles were determined to be monodispersed with the Fe mass determined to be 302 ± 53 fg *via* bulk-ICP-MS. The SP-ICP-TOF-MS results matched the bulk values and demonstrated a reproducible ^{56}Fe signal with 0.6% RSD over 10 injections during a ~4 h automated test. Subsequently, the binding performance of the H117G azurin functionalized microparticles was assessed and results showed that over 70% of microparticles measured had an associated Pt signal indicating that the metal was bound. The Pt bound to each individual azurin-coated microparticle was determined to be 0.32 ± 0.02 fg Pt per microparticle using SP-ICP-TOF-MS. These results were compared to results determined by bulk-digestion ICP-MS analysis and found to be consistently lower due to the ability to distinguish bound and free Pt. The capability of SP-ICP-TOF-MS analysis to be automated with proper attention to rinsing, mixing, and consistent injections will be essential for handling these larger sample population experiments. The SP-ICP-TOF-MS analysis procedure shown here demonstrates a new method with the potential for high-throughput quantification of the amount of metal bound to functionalized microparticles, which could be broadly implemented for other single particle applications.

The analysis presented here is not limited to the investigation of proteins and Pt. Of course, each component of the system, such as the particle, the method of attachment, the functional coating, and metals to be detected, can be leveraged for many applications. The magnetic microparticles characterized here offer a convenient means to isolate and amplify specific biological targets and are commonly used in isolation of any biotinylated or strep-tagged target. Accordingly, applications such as immunoassays, protein purification, cell isolation and identification, phage display, and biopanning are commonly employed with the magnetic particles characterized here. Given the wide prevalence of streptavidin/biotin functionalized molecules, as well as coated particles and surfaces, a plethora of application space is available. The work demonstrated here can be logically extended to an assortment of existing biological assays to leverage metal binding stoichiometry and the detection of unique metals to confirm the presence and quantity of a biological entities.

Conflicts of interest

L. H. works for TOFWERK AG.

Acknowledgements

This work was supported by the Laboratory Directed Research and Development Program of Oak Ridge National Laboratory, managed by UT-Battelle, LLC, for the U.S. Department of Energy under contract DE-AC-05-00OR22725. The authors would like to acknowledge Mark Boris for the assistance with optical images presented within this manuscript and Jacquelyn DeMink for assistance with graphics.

References

1 J. Zhang, M. P. Everson, T. J. Wallington, F. R. Field 3rd, R. Roth and R. E. Kirchain, Assessing Economic Modulation of Future Critical Materials Use: The Case of Automotive-Related Platinum Group Metals, *Environ. Sci. Technol.*, 2016, **50**(14), 7687–7695, DOI: **10.1021/acs.est.5b04654**.

2 S. Rottenberg, C. Disler and P. Perego, The rediscovery of platinum-based cancer therapy, *Nat. Rev. Cancer*, 2021, **21**(1), 37–50.

3 C.-J. Yang, An impending platinum crisis and its implications for the future of the automobile, *Energy Policy*, 2009, **37**(5), 1805–1808, DOI: **10.1016/j.enpol.2009.01.019**.

4 T. J. Wallington, E. W. Kaiser and J. T. Farrell, Automotive fuels and internal combustion engines: a chemical perspective, *Chem. Soc. Rev.*, 2006, **35**(4), 335–347, DOI: **10.1039/b410469m**.

5 M. Carmo, D. L. Fritz, J. Mergel and D. Stolten, A comprehensive review on PEM water electrolysis, *Int. J. Hydrogen Energy*, 2013, **38**(12), 4901–4934.

6 S. A. Singerling and R. F. Schulte, *Platinum-Group Metals*, U. S. G. S., 2018.

7 T. Maruyama, H. Matsushita, Y. Shimada, I. Kamata, M. Hanaki, S. Sonokawa, N. Kamiya and M. Goto, Proteins and protein-rich biomass as environmentally friendly adsorbents selective for precious metal ions, *Environ. Sci. Technol.*, 2007, **41**(4), 1359–1364.

8 E. Guibal, A. Larkin, T. Vincent and J. M. Tobin, Chitosan sorbents for platinum sorption from dilute solutions, *Ind. Eng. Chem. Res.*, 1999, **38**(10), 4011–4022.

9 C. Zhang, C. Xu, X. Gao and Q. Yao, Platinum-based drugs for cancer therapy and anti-tumor strategies, *Theranostics*, 2022, **12**(5), 2115.

10 S. R. McWhinney, R. M. Goldberg and H. L. McLeod, Platinum neurotoxicity pharmacogenetics, *Mol. Cancer Ther.*, 2009, **8**(1), 10–16.

11 D. Horak, M. Babič, H. Mackova and M. J. Beneš, Preparation and properties of magnetic nano-and microsized particles for biological and environmental separations, *J. Sep. Sci.*, 2007, **30**(11), 1751–1772.

12 K. Mehrabi, M. Dengler, I. Nilsson, M. Baumgartner, C. A. Mora, D. Gunther and A. Gundlach-Graham, Detection of magnetic iron nanoparticles by single-particle ICP-TOFMS: case study for a magnetic filtration medical device, *Anal. Bioanal. Chem.*, 2022, **414**(23), 6743–6751, DOI: **10.1007/s00216-022-04234-w**.

13 J. J. Zhang, C. Nie, W. L. Fu, F. L. Cheng, P. Chen, Z. F. Gao, Y. Wu and Y. Shen, Photoresponsive DNA-modified magnetic bead-assisted rolling circle amplification-driven visual photothermal sensing of Escherichia coli, *Anal. Chem.*, 2022, **94**(48), 16796–16802.

14 A. Ali, T. Shah, R. Ullah, P. Zhou, M. Guo, M. Ovais, Z. Tan and Y. Rui, Review on recent progress in magnetic nanoparticles: Synthesis, characterization, and diverse applications, *Front. Chem.*, 2021, **9**, 629054.

15 M. F. Hamza, A. Gamal, G. Hussein, M. S. Nagar, A. A. H. Abdel-Rahman, Y. Wei and E. Guibal, Uranium(VI) and zirconium(IV) sorption on magnetic chitosan derivatives – effect of different functional groups on separation properties, *J. Chem. Technol. Biotechnol.*, 2019, **94**(12), 3866–3882, DOI: **10.1002/jctb.6185**.

16 P. A. Vinosha, A. Manikandan, A. C. Preetha, A. Dinesh, Y. Slimani, M. A. Almessiere, A. Baykal, B. Xavier and G. F. Nirmala, Review on Recent Advances of Synthesis, Magnetic Properties, and Water Treatment Applications of Cobalt Ferrite Nanoparticles and Nanocomposites, *J. Supercond. Novel Magn.*, 2021, **34**(4), 995–1018, DOI: **10.1007/s10948-021-05854-6**.

17 S. Ojha, S. Chappa, A. M. Mhatre, K. K. Singh, V. Chavan and A. K. Pandey, Actinides selective extractants coated magnetite nanoparticles for analytical applications, *J. Radioanal. Nucl. Chem.*, 2017, **312**(3), 675–683, DOI: **10.1007/s10967-017-5246-6**.

18 A. R. Behnam-Saba, K. Saberyan, A. Nezhadali and H. Adelkhani, A Chemometric Study of the Adsorption of Zr(IV) Ions from Aqueous Solutions onto TBP-Surface-Modified Magnetic Fe3O4 Nanoparticles as a New Adsorbent, *Radiochemistry*, 2020, **62**(1), 62–72, DOI: **10.1134/s1066362220010087**.

19 B. Meermann and V. Nischwitz, ICP-MS for the analysis at the nanoscale – a tutorial review, *J. Anal. At. Spectrom.*, 2018, **33**(9), 1432–1468, DOI: **10.1039/c8ja00037a**.

20 M. D. Montaño, J. W. Olesik, A. G. Barber, K. Challis and J. F. Ranville, Single Particle ICP-MS: Advances toward routine analysis of nanomaterials, *Anal. Bioanal. Chem.*, 2016, **408**, 5053–5074.

21 D. M. Mitrano, E. K. Lesher, A. Bednar, J. Monserud, C. P. Higgins and J. F. Ranville, Detecting nanoparticulate silver using single-particle inductively coupled plasma-mass spectrometry, *Environ. Toxicol. Chem.*, 2012, **31**(1), 115–121, DOI: **10.1002/etc.719**.

22 H. E. Pace, N. J. Rogers, C. Jarolimek, V. A. Coleman, C. P. Higgins and J. F. Ranville, Determining transport efficiency for the purpose of counting and sizing nanoparticles *via* single particle inductively coupled plasma mass spectrometry, *Anal. Chem.*, 2011, **83**(24), 9361–9369.

23 L. Hendriks, A. Gundlach-Graham, B. Hattendorf and D. Günther, Characterization of a new ICP-TOFMS instrument with continuous and discrete introduction of

solutions, *J. Anal. At. Spectrom.*, 2017, **32**(3), 548–561, DOI: 10.1039/c6ja00400h.

24 M. Baalousha, J. Wang, M. Erfani and E. Goharian, Elemental fingerprints in natural nanomaterials determined using SP-ICP-TOF-MS and clustering analysis, *Sci. Total Environ.*, 2021, **792**, 148426, DOI: 10.1016/j.scitotenv.2021.148426.

25 A. Gondikas, F. von der Kammer, R. Kaegi, O. Borovinskaya, E. Neubauer, J. Navratilova, A. Praetorius, G. Cornelis and T. Hofmann, Where is the nano? Analytical approaches for the detection and quantification of TiO 2 engineered nanoparticles in surface waters, *Environ. Sci.: Nano*, 2018, **5**(2), 313–326.

26 L. G. Jahn, G. D. Bland, L. W. Monroe, R. C. Sullivan and M. E. Meyer, Single-particle elemental analysis of vacuum bag dust samples collected from the International Space Station by SEM/EDX and SP-ICP-ToF-MS, *Aerosol Sci. Technol.*, 2021, **55**(5), 571–585, DOI: 10.1080/02786826.2021.1874610.

27 L. Hendriks and D. M. Mitrano, Direct Measurement of Microplastics by Carbon Detection *via* Single Particle ICP-TOFMS in Complex Aqueous Suspensions, *Environ. Sci. Technol.*, 2023, **57**(18), 7263–7272.

28 S. Harycki and A. Gundlach-Graham, Characterization of a high-sensitivity ICP-TOFMS instrument for microdroplet, nanoparticle, and microplastic analyses, *J. Anal. At. Spectrom.*, 2023, **38**(1), 111–120.

29 B. T. Manard, V. C. Bradley, C. D. Quarles, L. Hendriks, D. R. Dunlap, C. R. Hexel, P. Sullivan and H. B. Andrews, Towards Automated and High-Throughput Quantitative Sizing and Isotopic Analysis of Nanoparticles *via* Single Particle-ICP-TOF-MS, *Nanomaterials*, 2023, **13**(8), 1322.

30 S. Naasz, S. Weigel, O. Borovinskaya, A. Serva, C. Cascio, A. K. Undas, F. C. Simeone, H. J. Marvin and R. J. Peters, Multi-element analysis of single nanoparticles by ICP-MS using quadrupole and time-of-flight technologies, *J. Anal. At. Spectrom.*, 2018, **33**(5), 835–845.

31 P. Menero-Valdés, M. I. Chronakis, B. Fernández, C. D. Quarles Jr, H. González-Iglesias, B. r. Meermann and R. Pereiro, Single Cell–ICP–ToF-MS for the Multiplexed Determination of Proteins: Evaluation of the Cellular Stress Response, *Anal. Chem.*, 2023, **95**(35), 13322–13329.

32 L. Hendriks, V. M. Kissling, T. Buerki-Thurnherr and D. M. Mitrano, Development of single-cell ICP-TOFMS to measure nanoplastics association with human cells, *Environ. Sci.: Nano*, 2023, 3439–3449.

33 S.-i. Miyashita, A. S. Groombridge, S.-i. Fujii, A. Minoda, A. Takatsu, A. Hioki, K. Chiba and K. Inagaki, Highly efficient single-cell analysis of microbial cells by time-resolved inductively coupled plasma mass spectrometry, *J. Anal. At. Spectrom.*, 2014, **29**(9), 1598–1606.

34 M. Corte-Rodríguez, R. Álvarez-Fernández, P. García-Cancela, M. Montes-Bayón and J. Bettmer, Single cell ICP-MS using on line sample introduction systems: Current developments and remaining challenges, *TrAC, Trends Anal. Chem.*, 2020, **132**, 116042.

35 J. R. Winkler and H. B. Gray, Electron transfer in ruthenium-modified proteins, *Chem. Rev.*, 1992, **92**(3), 369–379.

36 N. M. Marshall, D. K. Garner, T. D. Wilson, Y.-G. Gao, H. Robinson, M. J. Nilges and Y. Lu, Rationally tuning the reduction potential of a single cupredoxin beyond the natural range, *Nature*, 2009, **462**(7269), 113–116.

37 J.-W. Choi, B.-K. Oh, Y. J. Kim and J. Min, Protein-based biomemory device consisting of the cysteine-modified azurin, *Appl. Phys. Lett.*, 2007, **91**(26), 263902.

38 M. P. McLaughlin, T. H. Darrah and P. L. Holland, Palladium(II) and platinum(II) bind strongly to an engineered blue copper protein, *Inorg. Chem.*, 2011, **50**(22), 11294–11296, DOI: 10.1021/ic2017648.

39 A. Gundlach-Graham, L. Hendriks, K. Mehrabi and D. Günther, Monte Carlo simulation of low-count signals in time-of-flight mass spectrometry and its application to single-particle detection, *Anal. Chem.*, 2018, **90**(20), 11847–11855.

40 M. von der Au, M. Schwinn, K. Kuhlmeier, C. Büchel and B. Meermann, Development of an automated on-line purification HPLC single cell-ICP-MS approach for fast diatom analysis, *Anal. Chim. Acta*, 2019, **1077**, 87–94.

41 F. Laborda, C. Trujillo and R. Lobinski, Analysis of microplastics in consumer products by single particle-inductively coupled plasma mass spectrometry using the carbon-13 isotope, *Talanta*, 2021, **221**, 121486.